Nanoparticle loaded implantable flexible microelectrode arrays for pain management after spinal cord surgery

Nuo Xu

A thesis

Submitted in partial fulfillment of the

Requirements for the degree of

Master of Science

University of Washington

2021

Committee:

Elizabeth Nance

Lilo Pozzo

Program Authorized to Offer Degree:

Chemical Engineering

University of Washington

Abstract

Nanoparticle loaded implantable flexible microelectrode arrays for pain management after spinal cord surgery

Nuo Xu

Chair of the Supervisory Committee:

Elizabeth Nance

Department of Chemical Engineering

The health care system currently faces significant burden with abuse of opioids and an unmet market need for pain management after surgery and injury. A drug delivery device that can improve drug delivery efficiency, increase drug duration of action, and deliver anesthetics topically with low toxicity is needed. Implantable flexible microelectrode arrays are widely used after spinal cord injury for pain mainagement, but they have limitations in improving the solubility, bioavailability, and permeability of drug. Biodegradable polymeric nanoparticles have highly tailorable physicochemical properties, and with incorporation on microelectrode arrays (MEAs), may increase the physical and chemical properties of therapeutic agents such as permeability, solubility and bioavailability. However, drug-loaded biodegradable nanoparticle-polypyrrole coated MEA for drug delivery has not been reported in literature. Therefore, we investigate the use of biodegradable nanoparticles for controlled release of bupivacaine hydrochloride from MAEs for pain management following spinal cord surgery. Bupivacaine hydrochloride, a commonly used FDA-approved anesthetic, is chosen as the model drug due to its nerve block and anti-inflammatory effects. This work starts with the exploration of the relationship between the formulation parameters of biodegradable nanoparticles and their physicochemical properties. Then, the bupivacaine hydrochloride loaded nanoparticles are formulated, and the drug loading of the nanoparticles is explored through iterating formulation parameters. Thereafter, nanoparticles with different surface charges are loaded on the MAEs to determine the relationship between the surface charge of nanoparticles and the release behavior of these nanoparticles. Finally, the release behavior of the nanoparticles from the MAEs is used as a guide to further optimize the bupivacaine hydrochloride loaded nanoparticle formulation.

TABLE OF CONTENTS

LIST OF FIGURES

LIST OF TABLES

ACKNOWLEDGEMENT

First, I would like to thank my advisor, Dr. Elizabeth Nance, for her research and future path advice and support, and giving me the opportunity to work in her lab. I really appreciate her for mentoring my research project, thesis, and being a role model as a researcher. I applied to graduate school because I wanted to conduct research in the interdisciplinary fields of engineering and pharmacy. Nance lab is an ideal place to combine the interface of chemical engineering, neuroscience, and nanomedicine, allowing me to gradually approach my career goal to become a research scientist in the field of biomedicine. I also would like to thank Dr. Lilo Pozzo for reading my thesis.

I would like to thank the entire Nance lab family for the consistent support and welcoming environment, and especially Andrea, Megan, and the entire therapeutics subgroup. Thank you Andrea for providing comprehensive training to make everything in lab so easy to learn, and thank you for your continued support and willingness to help. Thank you Megan for your trust and help, you let me enjoy my first mentoring experience, I am grateful for what I have learned in mentoring.

I would like to thank my mom and dad for supporting me throughout life, and my best friends Yue and Difan for being there for me through the ups and downs. The past year is a weird year due to the covid pandemic, I really appreciate your support during this period, especially the shut down time. The happy time I spent with you through video calls made me feel that I was not alone in the three months I worked at home.

Thank you all for the love and support over the past two years of my MS studies.

CHAPTER 1: Introduction

1.1 Clinical unmet need for low-toxic local anesthesia

Approximately 51 million Americans undergo inpatient surgery annually and pain management is often needed after surgery.[1-4] Acute postoperative pain is a common and challenging problem, usually occurring within 48 hours after surgery, and can delay recovery and develop into chronic pain. The current postoperative analgesia regimens constitute multimodal approaches, with combinations of acetaminophen, nonsteroidal anti-inflammatory agents, steroids and oral or parenteral opioids, and pain management can be categorized as systemic or local.[2, 5] In systemic treatments, such as with oral or intravenous opioids (or acetaminophen), the drug courses throughout the body, and has most of its effects in the central nervous system. However, systemic treatments (especially opioids) tend to have many side effects: constipation, urinary retention, itchiness, and perhaps more seriously, sedation, addiction/tolerance, and death from overdose.[2] Moreover, opioids are the primary modality for postoperative acute pain management. Over 80% of patients receive opioids after low-risk surgery, and opioid prescribing has quadrupled since 1999, and has risen in parallel with the number of overdoses from the most commonly prescribed opioids. The economic cost of prescription opioid-related overdose, abuse and dependence exceeds $78.5 billion annually with the majority of costs related to health care, substance abuse treatment, and lost productivity.[2, 4] Therefore, there is still unmet clinical need for the strategies of the topical delivery of the numbing medicine with low toxicity, and strategies that can improve drug delivery efficiency and increase drug duration of action will allow for a broader approach to acute postoperative pain management by achieving improved drug bioavailability and controlled drug release characteristics to the target site of action.

1.2 Role of local anesthesia in pain management

In local anesthesia, local anesthetics that affect axonal impulse conduction are deposited at the desired site of action, interrupting the transmission of pain signals to the central nervous system. This can be applied by injection throughout a tissue to be affected, known as infiltration anesthesia, or on a specific peripheral nerve leading to anesthesia of all downstream structures such as peripheral nerve blocks, or on or around the spinal cord such as with spinal and epidural blocks.[2] Therefore, the dose of anesthetics can be much lower than the dose required for systemic anesthesia. However, owing to the low molecular weight of anesthetics, the duration of the analgesia induced by a single injection is usually only a few hours, which does not meet the requirements for most clinical applications. The conventional approach to achieve prolonged analgesia is the continuous infusion of anesthetics through a catheter. Although this approach does relieve pain, it suffers from some

limitations such as high cost, high technical requirements, and complications.[1] Thus, there is a need for the development of local anesthetic formulations with longer-lasting effects that can be administered as a single dose.

1.3 Bupivacaine as a local anesthetic agent

Bupivacaine (BUP) is an amino-amide local anesthetic, which acts by inactivating voltage-dependent sodium channels. Protonation under acidic pH secondary and tertiary amines in amino-amides (with a pKa of 7 - 8) renders the drugs hydrophilic. BUP has a pKa of 8.1 so only 15% is present in uncharged form at tissue pH. The uncharged fraction of BUP travels across the cell membrane of the nerve, and once charged binds to the inner side of sodium channels, inactivating them. Thus, BUP is usually used in the form of bupivacaine hydrochloride preparations (BUP·HCl). The release of BUP from its binding site is slow, which leads to a longer duration of action than lidocaine.[1, 4, 6] Furthermore, BUP inhibits synaptic N-methyl-D-aspartate receptors and has anti-inflammatory properties.[7, 8] The anesthetic agent decreases the expression of nuclear factor (NF)-κB and proinflammatory cytokines such as tumor necrosis factor-α (TNF-α), interleukin-1β (IL-1β) and interleukin-6 (IL-6), and the decreased activation of microglia and astrocytes was observed in rat models of inflammatory pain after BUP treatment.[9, 10] However, the effects of local anesthetics are generally relatively short in duration, lasting for several hours after a single injection, which is inadequate for the treatment of prolonged acute pain and chronic pain. In such instances, achieving prolonged sensory nerve blockade, lasting days to weeks, is desirable. In addition, the high volume of BUP can cause side effects and toxicity.[11, 12] Therefore, low dose, sustained release of BUP has significant potential for ameliorating ongoing postoperative pain. One avenue of investigation has focused on encapsulating local anesthetics within carrier molecules to increase their residence time at the site of action.[6]

1.4 Implantable flexible microelectrode arrays

Electrical stimulation and recording are widely used as therapeutic and monitoring methods after nervous system injuries.[13, 14] Implantable microelectrode array (MEA) are one type of implantable medical device, which can selectively stimulate neurons and then record the responses of them - thus MEA can also help understand the dynamics of neutral networks.[13, 15-18] Polypyrrole is a conducting polymers that has many unique properties, including reversible mechanical behavior, high electrical conductivity, satisfactory biocompatibility, and ability to change porosity and volume in response to applied electrochemical stimuli, which makes it an effective and minimally invasive material for coating onto the implantable MEAs.[17, 19, 20] Moreover, it has been

reported that polypyrrole based materials exhibit a level of immunogenicity comparable to other FDA-approved biomaterials.[21] Thus, polypyrrole MEA is an electronically controlled implantable drug delivery device with good biocompatibility that has potential to deliver drug to the site of action. However, potential limitations should still be bridged between the device itself and its clinical applications. The first limitation is the tissue or cell penetration of therapeutic agents released from the MEA. Many free drugs have limited permeability and solubility, but MEA cannot alter the physical and chemical properties of drugs. Additionally, the polypyrrole-drug coating requires the specific electrochemical properties of the loaded drug, which also increases the difficulty of free drug to be coated on the MEAs. Based on the limitations of the MEA device and the free drugs, a bridge agent with highly tailorable physicochemical properties is required.

1.5 Biodegradable polymeric nanoparticles coated on MEAs for local topical delivery

Biodegradable polymeric nanoparticles are frequently used to improve the therapeutic value of various water soluble/insoluble medicinal drugs and bioactive molecules by improving bioavailability, solubility, and retention time. The nanoparticle–drug formulation reduces patient expenses and risk of toxicity. Nanoencapsulation of medicinal drugs (nanomedicines) increases drug efficacy, specificity, tolerability and therapeutic index of corresponding drugs.[11] In addition, drug release rates from the polymeric nanoparticles can be controlled by modifying polymer chemical and physical properties.[12] Therefore, we propose that biodegradable polymeric nanoparticles loaded with BUP·HCl can be loaded on MEAs with polypyrrole to achieve sustained, controlled, and local drug release.

CHAPTER 2: Methods

2.1 Nanoprecipitation technique

The nanoprecipitation technique was used for blank nanoparticles with different size and/or surface charge preparation, and curcumin encapsulation. mPEG-PLGA (5,000:45,000 Da, 50:50 LA:GA, Akina) or PLGA (Mn 35,000-45,000 Da, 50:50 LA:GA, Akina) polymer was dissolved in 1 mL acetone (Fisher Scientific) with curcumin (Sigma-Aldrich). The polymer solution (organic phase) was then added dropwise into 25 mL of surfactant solution (sink), where nanoparticles formed spontaneously, and were stirred for 3 h at 500 rpm to remove the organic solvent. Nanoparticles were collected and washed twice by ultracentrifugation with deionized (DI) water at 100,000 $\times g$. Finally, the nanoparticles were resuspended in 1 mL of DI water, or 1 × phosphate buffered saline (PBS). Nanoparticles were used immediately or were lyophilized with 20% (w/v) sucrose added as a cryoprotectant and stored at −80°C until further use.

2.2 Emulsion-solvent evaporation technique

The emulsion-solvent evaporation technique was used for bupivacaine hydrochloride (BUP·HCl, Sigma-Aldrich) encapsulation, all the nanoparticles were prepared using single emulsion and double emulsion with 20% or 30% amplitude, and 10s or 30s emulsification time.

2.2.1 Single emulsion method

mPEG-PLGA or PLGA polymer was dissolved in 1 mL dichloromethane (DCM, Fisher Scientific) with BUP·HCl. The polymer solution (organic phase) was added into 4 mL surfactant solution (water phase) and then emulsified with a Sonic Dismembrator Ultrasonic Processor (model FB505, Fisher Scientific). The emulsion was then poured into 25 mL of surfactant solution, and was stirred for 3 h at 500 rpm to remove the organic solvent. Nanoparticles were collected and washed twice by ultracentrifugation with DI water at 100,000 × g. Finally, the nanoparticles were resuspended in 1 mL of DI water, or 1 × phosphate buffered saline. Nanoparticles were used immediately or were lyophilized with 20% (w/v) sucrose added as a cryoprotectant and stored at −80°C until further use.

2.2.2 Double emulsion method

mPEG-PLGA or PLGA polymer was dissolved in 1 mL dichloromethane (organic phase), BUP·HCl was dissolved in 0.2 mL surfactant solution (w1 phase). The organic phase was added into w1 phase and then emulsified with a Sonic Dismembrator Ultrasonic Processor (model FB505, Fisher Scientific). Then 4 mL surfactant solution (w2 phase) was added into the emulsion, followed by a second emulsification with the Sonic Dismembrator Ultrasonic Processor. The emulsion was then poured into 25 mL of surfactant solution, and was stirred for 3 h at 500 rpm to remove the organic solvent.

Nanoparticles were collected and washed twice by ultracentrifugation with DI water at 100,000 × g. Finally, the nanoparticles were resuspended in 1 mL of DI water, or 1 × phosphate buffered saline. Nanoparticles were used immediately or were lyophilized with 20% (w/v) sucrose added as a cryoprotectant and stored at −80°C until further use.

2.3 Particle size, polydispersity index (PDI), and zeta potential

The particle size and PDI of the blank and drug loaded nanoparticles were measured by dynamic light scattering (DLS), and the zeta potential (ζ-potential) was determined using a zeta potential analyzer (NanoSizer Zeta Series, Malvern Instruments, Malvern, UK). Samples were diluted to appropriate concentrations to obtain accurate measurements in 10 mM sodium chloride (NaCl), pH 7.4, as described elsewhere.[22]

2.4 Drug loading and encapsulation efficiency

Drug loading (DL) and drug encapsulation efficiency (DEE) are defined as follows:

$$\text{Drug loading (\%)} = \frac{Weight\ of\ drug\ encapsulated\ in\ nanoparticles}{Total\ weight\ of\ nanoparticles} \times 100\%$$

$$\text{Drug encapsulation efficiency (\%)} = \frac{Weight\ of\ drug\ encapsulated\ in\ nanoparticles}{Total\ weight\ of\ drug\ used\ in\ formulation} \times 100\%$$

2.4.1 Curcumin loading and encapsulation efficiency

Drug loading and encapsulation efficiency were determined by ultraviolet–visible light (UV–Vis, SpectraMax M5, Molecular Devices) spectrometer as compared to a standard calibration curve of curcumin in DMSO. Each sample's absorbance at 430 nm was measured and adjusted by subtracting a blank of unloaded polymer nanoparticles' absorbance in DMSO. The weight of a polymer and drug was determined by lyophilizing the nanoparticle sample.

2.4.2 BUP·HCl loading and encapsulation efficiency

Drug loading and encapsulation efficiency were determined indirectly by determining the amount of drug remaining in the supernatant after loading, by Agilent 8453 UV-Vis spectrometer (Agilent Technologies) as compared to a standard calibration curve of BUP·HCl.[23] Each sample's absorbance at 263 nm was measured and adjusted by subtracting the absorbance of the unloaded polymer nanoparticles' supernatant. Additionally, BUP·HCl loaded nanoparticles were lyophilized, redissolved, and stirred in chloroform overnight, then extracted with distilled water and quantified using Agilent 8453 UV-Vis spectrometer at 263 nm to determine drug loading as well.[24]

2.5 *In-vitro* drug release

Curcumin loaded nanoparticles were resuspended in 1 mL PBS, BUP·HCl loaded nanoparticles were resuspended in 1 mL DI water. Each sample was evenly distributed to three dialysis tubing cellulose ester membranes (MWCO: 300kDa, Spectrum Laboratories). The membranes were submerged in 25 mL PBS (curcumin loaded nanoparticles) or DI water (BUP·HCl loaded nanoparticles) and were placed on a shaker at 60 rpm at 37°C. At designated time points, the membranes were transferred to fresh 25 mL PBS. From the supernatants collected at each time point, curcumin or BUP·HCl content was determined by SpectraMax M5 UV-Vis spectrometer or Agilent 8453 UV-Vis spectrometer. Percent curcumin or BUP·HCl released from the nanoparticles was defined as the curcumin or BUP·HCl amount released at a specific time point divided by the total curcumin or BUP·HCl encapsulated in the nanoparticles.

2.6 Polymer labeling method

Blank PLGA and mPEG-PLGA nanoparticles were labeled with fluorescence dye to explore nanoparticle loading and release behaviors from polypyrrole MEAs, described below.

2.6.1 Polymer activation

PLGA and mPEG-PLGA polymers were dissolved in a 20mL glass scintillation vial in specified amount of DCM. P-nitrophenyl chloroformate (PNCF, Sigma-Aldrich) was dissolved in DCM to make a 10 mg/mL stock solution. Exact amount of PNCF solution was added to polymer solution, and then pyridine was added immediately. Stirred and reacted for 3 h at 200-300rpm. A tube was filled with 5 times of the reaction volume of cold ethyl ether, and then the polymer reaction solution was slowly added dropwise to the cold ethyl ether in the tube. Centrifuged at 1000 × *g* for 2 min, then the ethyl ether was decanted into an ethyl ether waste. Once all ether was decanted, the tube was transported to lyophilizer and set overnight. After lyophilization, the tube was weighed and the initial weight of tube was subtracted from the new tube weight.

2.6.2 Conjugation of fluorescence dye to activated polymer

CF555 Succinimidyl Ester (CF555, Biotium) was dissolved in DMF to make 2mg/mL stock solution. Activated polymer was dissolve in DMF, and then the CF555 solution was added in. Triethylamine (TEA) was added. Reacted for 4 h. A tube was filled with 5 times of the reaction volume of cold ethyl ether, and then the polymer reaction solution was slowly added dropwise to the cold ethyl ether in the tube. Centrifuged at 1000 × *g* for 2 min, then the ethyl ether was decanted into an ethyl ether waste. Once all ether was decanted, the tube was transported to lyophilizer and set overnight.

CHAPTER 3: PLGA nanoparticles with different size and surface charge

3.1 Introduction

Particle size and surface charge are two fundamental physicochemical properties, which play an important role in nanoparticles' permeability, diffusivity, cellular uptake rate, biodistribution, systemic circulation, elimination, and toxicity.[25-27] Drug loaded nanoparticles with different size and surface charge have been applied in various therapeutic applications to achieve skin or mucous penetration and retention, reduced clearance and toxicity modulation, cell or tissue targeting, and increased site specific uptake.[28-34] Size and surface charge are key parameters for nanoparticle formulation, and they can be tailored to accomplish the requirements of drug delivery applications such as targeting, permeability and cellular uptake.

In this chapter, size and surface charge of PLGA nanoparticles are the two main properties to explore. There are two main goals: One is to establish the relationship between the size and surface charge of nanoparticles and PLGA concentration and different surfactants; the other is to formulated PLGA nanoparticles with controlled surface charge, ranging from near neutral to high negative, where the particle size difference is within 10 nm. These results will provide a foundation for further exploration of the relationship between the properties of nanoparticles and nanoparticle loading and release behaviors from MEAs, which will be further discussed in Chapter 5. Additionally, curcumin was chosen as a model drug to demonstrate the drug release behaviors from MEAs (Chapter 5) because its natural fluorescence allows for UV-vis spectroscopy readouts without additional fluorophore conjugations. In this chapter, curcumin will be added in the finalized formulations and then characterized, in order to verify drug-loaded particle size differences are within 10 nm and surface charges are as expected.

3.2 Results

3.2.1 Effect of different surfactants on the size and surface charge of PLGA nanoparticles prepared by nanoprecipitation method

Blank PLGA (45k, 50:50) nanoparticles were formulated using 20 mg polymer and 2% polyvinyl alcohol (PVA, 27k, Sigma-Aldrich), 1% Pluronic F127 (F127, Sigma-Aldrich), 1% Polysorbate 80 (P80, Sigma-Aldrich), 3% cholic/deoxycholic acid sodium salt (CHA, bile salts, Sigma-Aldrich), 5% Pluronic F68 (F68, Sigma-Aldrich), or 2% sodium dodecylbenzenesulfonate (NaDBS, Sigma-Aldrich). All the nanoparticles were prepared by nanoprecipitation method, as described in Chapter 2.1. The particle size, PDI, and zeta potential of the nanoparticles are listed in Table 3-1.

Table 3-1 Blank PLGA nanoparticles prepared with different surfactants

Polymer concentration (mg/mL)	Surfactant	Number Mean ± SEM (nm)	PDI ± SEM	Zeta Potential ± SEM (mV)
20	2% PVA	62.79 ± 2.09	0.264 ± 0.007	-3.58 ± 0.71
20	1% F127	90.44 ± 0.61	0.082 ± 0.082	-5.90 ± 0.40
20	1% P80	81.77 ± 0.69	0.162 ± 0.001	-11.14 ± 5.27
20	3% CHA	111.13 ± 7.22	0.147 ± 0.006	-45.30 ± 2.03
20	5% F68	91.13 ± 3.34	0.183 ± 0.021	-15.30 ± 4.83
20	2% NaDBS	113.83 ± 3.33	0.143 ± 0.034	-61.77 ± 2.81

Data are presented as average of N ≥3 batches. SEM: standard error of measurement

3.2.2 Effect of PLGA concentrations on the size and surface charge of PLGA nanoparticles

Based on the results shown in Table 3-1, PLGA nanoparticles formulated with 2% PVA, 5% F68, and 3% CHA were chosen as near neutral, negative, and high negative PLGA nanoparticles, respectively. Different PLGA concentrations were iterated in these three formulations to study the effect of polymer concentration on the nanoparticle properties.

3.2.2.1 PLGA nanoparticles prepare with 2% PVA

Nanoparticles were formulated using nanoprecipitation method with 2% PVA and 10 mg/mL, 20 mg/mL, or 40 mg/mL PLGA dissolved in acetone. Each formulation was prepared in triplicate, and then characterized within 24 h after formulation. The particle size, PDI, and zeta potential of the nanoparticles are listed in Table 3-2.

Table 3-2 Blank PLGA nanoparticles prepared with different PLGA concentrations and 2% PVA

Polymer concentration (mg/mL)	Surfactant	Number Mean ± SEM (nm)	PDI ± SEM	Zeta Potential ± SEM (mV)
10	2% PVA	57.37 ± 8.83	0.331 ± 0.011	-3.32 ± 0.43
20	2% PVA	62.79 ± 2.09	0.264 ± 0.007	-3.58 ± 0.71
40	2% PVA	78.69 ± 21.20	0.293 ± 0.032	-6.32 ± 1.38

Data are presented as average of N = 3 batches. SEM: standard error of measurement

3.2.2.2 PLGA nanoparticles prepare with 3% CHA

Nanoparticles were formulated using nanoprecipitation method with 3% CHA and 10 mg/mL, 20 mg/mL, or 40 mg/mL PLGA dissolved in acetone. Each formulation was prepared in triplicate, and then characterized within 24 h after formulation. The particle size, PDI, and zeta potential of the nanoparticles are listed in Table 3-3.

Table 3-3 Blank PLGA nanoparticles prepared with different PLGA concentrations and 3% CHA

Polymer concentration (mg/mL)	Surfactant	Number Mean ± SEM (nm)	PDI ± SEM	Zeta Potential ± SEM (mV)
10	3% CHA	97.57 ± 9.30	0.177 ± 0.034	-33.83 ± 3.70
20	3% CHA	111.13 ± 7.22	0.147 ± 0.006	-45.30 ± 2.03
40	3% CHA	128.00 ± 5.21	0.231 ± 0.015	-62.03 ± 2.08

Data are presented as average of N = 3 batches. SEM: standard error of measurement

3.2.2.3 PLGA nanoparticles prepare with 5% F68

Nanoparticles were formulated with 5% F68 by nanoprecipitation method and single emulsion method. For the nanoprecipitation method, 10 mg/mL, 20 mg/mL, or 40 mg/mL PLGA was dissolved in acetone. For the single emulsion method, 20 mg/mL, 35 mg/mL, or 50 mg/mL PLGA was dissolved in DCM. Each formulation was prepared in triplicate, and then characterized within 24 h after formulation. The particle size, PDI, and zeta potential of the nanoparticles prepared by nanoprecipitation method (Table 3-4) and single emulsion method (Table 3-5) are shown below.

Table 3-4 Blank PLGA nanoparticles prepared with different PLGA concentrations and 5% F68 by nanoprecipitation method

Polymer concentration (mg/mL)	Surfactant	Number Mean ± SEM (nm)	PDI ± SEM	Zeta Potential ± SEM (mV)
10	5% F68	67.92 ± 8.01	0.233 ± 0.036	-7.83 ± 0.41
20	5% F68	91.13 ± 3.34	0.183 ± 0.021	-15.30 ± 4.83
40	5% F68	116.90 ± 7.22	0.230 ± 0.006	-24.13 ± 2.03

Data are presented as average of N = 3 batches. SEM: standard error of measurement

Table 3-5 Blank PLGA nanoparticles prepared with different PLGA concentrations and 5% F68 by single emulsion method

Polymer concentration (mg/mL)	Surfactant	Number Mean ± SEM (nm)	PDI ± SEM	Zeta Potential ± SEM (mV)
20	5% F68	129.83 ± 9.45	0.217 ± 0.040	-22.97 ± 2.42
35	5% F68	157.03 ± 4.04	0.222 ± 0.011	-29.37 ± 2.06
50	5% F68	90.69 ± 32.67	0.166 ± 0.011	-41.70 ± 0.71

Data are presented as average of N = 3 batches. SEM: standard error of measurement

3.2.2.4 Relationship between PLGA concentration and size and surface charge of nanoparticles

The relationships between PLGA concentration and particle size and surface charge of PLGA nanoparticles were further analyzed through plotting and comparing the nanoparticle properties with different PLGA concentrations and surfactants (Figure 3-1).

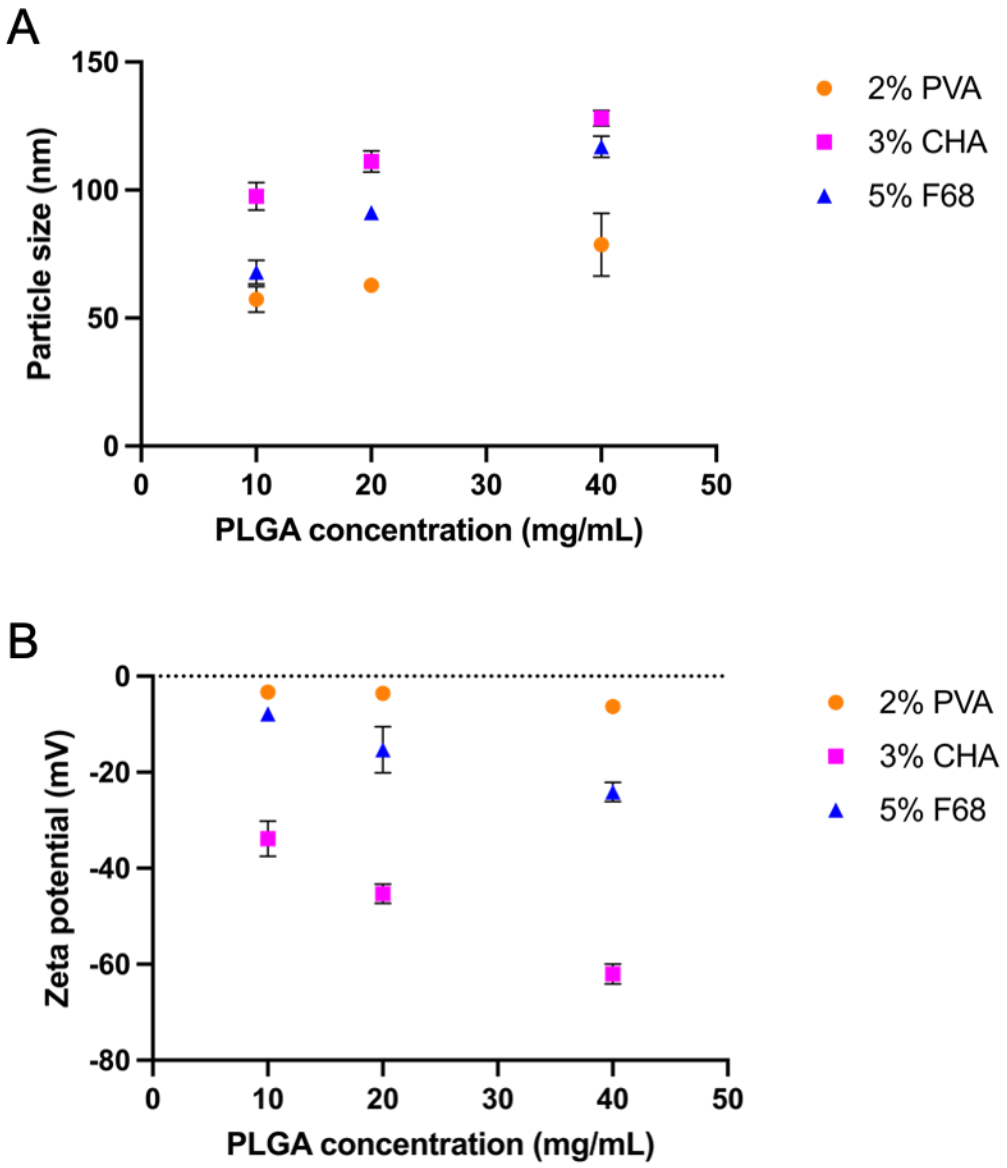

Figure 3-1 Relationship between PLGA concentration and size and surface charge of nanoparticles. Polymer concentrations were varied from 10 to 40mg/mL and formulated in 2% PVA, 3% CHA, and 5% F68. A) Independent of surfactant, particle concentration shows a linear relationship to particle size (R^2 = 0.99 for 2% PVA, R^2 = 0.98 for 3% CHA, R^2 = 0.99 for 5% F68). B) The relationship between polymer concentration and net surface charge, as measured by zeta potential, is highly correlated (R^2 = 0.94 for 2% PVA, R^2 = 0.99 for 3% CHA, R^2 = 0.98 for 5% F68). N = 3 batches per sample.

3.2.2.5 Curcumin loaded PLGA nanoparticles with similar size and different surface charge

According to Figure 3-1, size and surface charge of PLGA nanoparticles have a linear relationship with polymer concentration in the range of 10 mg to 40 mg. PLGA nanoparticles formulated with 40

mg PLGA and 2% PVA, 20 mg PLGA and 5% F68, and 10 mg PLGA and 3% CHA were chosen to represent PLGA nanoparticles with near neutral, negative, and high negative surface charge, respectively. To further verify the properties of PLGA nanoparticles will not change with curcumin loaded in, 10% (w/w) curcumin was added in these three formulations, and then characterized within 24 h after formulation. The particle size, PDI, and zeta potential of the nanoparticles are listed in Table 3-6.

Table 3-6 Curcumin-loaded PLGA nanoparticles prepared with 2% PVA, 5% F68, and 3% CHA

Polymer concentration (mg/mL)	Surfactant	Number Mean ± SEM (nm)	PDI ± SEM	Zeta Potential ± SEM (mV)
40 [a]	2% PVA	76.37 ± 0.24	0.453 ± 0.036	-1.20 ± 0.70
20 [b]	5% F68	84.55 ± 0.88	0.279 ± 0.055	-16.71 ± 1.26
10 [c]	3% CHA	86.05 ± 8.13	0.161 ± 0.016	-43.04 ± 5.82

[a] Data are presented as average of N = 2 batches. [b] Data are presented as average of N = 3 batches. [c] Data are presented as average of N = 6 batches. SEM: standard error of measurement

3.3 Discussion

In this chapter, the effects of different surfactants on the size and surface charge of PLGA nanoparticle were explored. Six different surfactants were added into the formulation: PVA is a hydrophilic polymer, P80, F127, and F68 are nonionic polymers, CHA and NaDBS are salts with small molecular weights. PLGA nanoparticles prepared with 2% PVA have the smallest size and closest near neutral surface charge. Additionally, they also have the most similar size to mPEG-PLGA (5k:45k) nanoparticles prepared without surfactant using the same protocol (61.975±0.90 nm, $p > 0.05$). One potential explanation is that PVA acts as a hydrophilic shell outside the hydrophobic PLGA core, and PLGA nanoparticles formulated with 2% PVA have a similar structure to mPEG-PLGA nanoparticles because both PEG and PVA are hydrophilic. However, compared to the molecular weight of PEG in the mPEG-PLGA (5k:45k) copolymer, the molecular weight of PVA (27k) is higher, which may explain why PLGA nanoparticles prepared with 2% PVA have a more neutral surface charge than mPEG-PLGA nanoparticles (-6.085±0.605 mV, $p < 0.05$). Formulations that use small molecule salt, such as 3% CHA and 2% NaDBS, resulted in larger particle sizes and more negative surface charges. This is probably due to the small molecule salt incorporation into the PLGA core instead of forming a hydrophilic corona outside the PLGA core. Compared with the batches prepared with 2% PVA, more aggregates were also observed in the batches of PLGA nanoparticles prepared with 3% CHA and 2%

NaDBS. This also supports the explanation that a hydrophilic PVA corona will form on the outside of the hydrophobic PLGA core, and this corona will stabilize the PLGA nanoparticles at the same time. Beside these three formulations, the size and surface charge of PLGA nanoparticles prepared with 1% F127, 1% P80, and 5% F68 are somewhere in between. Moreover, PLGA nanoparticles prepared with F127, P80, and F68 have more aggregates than the batches formulated with 2% PVA, but less than the batches formulated with 3% CHA and 2% NaDBS. The molecular weights of F127, P80, and F68 surfactants are between 1k and 4k, so they may form hydrophilic coronas with lower surface density than PVA. Considering the range of the particle size and surface charge, as well as the stability of the nanoparticles, this assumption is reasonable.

Formulations using 2% PVA, 5% F68, and 3% CHA are chosen for further exploration, because they represent PLGA nanoparticles with near neutral, negative, and high negative surface charges, respectively. In order to reduce the effect of particle size on its loading and release behavior, PLGA concentration is another variable to be studied in this chapter. The relationship between PLGA concentration and particle size and surface charge of PLGA nanoparticles can provide a guide for precise size and surface charge control. The effect of PLGA concentration on the particle size and surface charge are presented in Figure 3-1. Three concentrations of PLGA were used in these three formulations: 10 mg/mL, 20 mg/mL, and 40 mg/mL, and all the nanoparticles were prepared by the nanoprecipitation method. In these formulations, particle size and net surface charge of PLGA nanoparticles increased proportionally to PLGA concentration. The fitting of the experimental results shows that the particle size (D) and the PLGA concentration (C) have a linear relationship, and there is also a linear relationship between the surface charge (ζ) and the PLGA concentration (C). The size relationship of 2% PVA group follows the equation $D = 0.7224C + 49.43$, with the coefficient of determination $R^2 = 0.9925$. The size relationships of 3% CHA group and 5% F68 group follow the equations $D = 0.99C+89.133$, with the coefficient of determination $R^2 = 0.9838$, and $D = 1.6003C+53.857$, with the coefficient of determination $R^2 = 0.9891$, respectively. The zeta potential relationships of 2% PVA group, 3% CHA group, and 5% F68 group are $\zeta = -0.1052C-1.95$, with the coefficient of determination $R^2 = 0.9373$, $\zeta = -0.9252C-25.467$, with the coefficient of determination $R^2 = 0.9932$, and $\zeta = -0.529C-3.41$, with the coefficient of determination $R^2 = 0.98$, respectively. The sizes of these three series of PLGA nanoparticles overlapped in the range of 70 nm to 100 nm. To minimize the difference in particle size between each formulation, PLGA nanoparticles prepared with 40 mg/mL PLGA and 2% PVA (78.69 ± 21.20 nm, -6.32 ± 1.38 mV), 20 mg/mL PLGA and 5% F68 (91.13 ± 3.34 nm, -15.30 ± 4.83 mV), and 10 mg/mL PLGA and 3% CHA (97.57 ± 9.30 nm, -33.83 ± 3.70 mV) are selected as near neutral, negative, and high negative charged PLGA nanoparticles,

respectively. The calculated probability between the size of PLGA nanoparticles formulated with 40 mg/mL PLGA and 2% PVA, PLGA nanoparticles formulated with 20 mg/mL and 5% F68, and PLGA nanoparticles formulated with 10 mg/mL PLGA and 3% CHA are 0.246, 0.217, and 0.231, respectively, which shows the size differences are not obvious. The linear relationship between size and surface charge of PLGA nanoparticles and PLGA concentration when the PLGA concentration is between 10 mg/mL - 40 mg/mL may be due to the fact that PLGA concentration is the decisive variable for particle size and surface charge in the low PLGA concentration range. Therefore, all the PLGA polymers can quickly form nanoparticles after drop-wise addition into the sink. As a result, the higher the PLGA concentration, the larger the particles size and the more the net surface charges. However, as the concentration of PLGA increases, it will reach a critical point. Thereafter, the sink condition will replace PLGA concentration as the decisive variable, because the PLGA concentration in a droplet is greater than the maximum amount of PLGA that can form nanoparticles in the sink. This is one possible reason for why the particle size (146.15 nm) and surface charge (-10.97 mV) of PLGA nanoparticles formulated with 200 mg/mL PLGA and 2% PVA were not as high as those calculated (194.13 nm and -22.99 mV) using the equations from 10 mg/mL to 40 mg/mL. The particle size (127.04nm) and surface charge (-13.76 mV) of PLGA nanoparticles prepared with 100 mg PLGA and 5% F68 were also not the same as they were predicted by the equations (213.88 nm and -56.31 mV).

Unlike the PLGA nanoparticles formulated using nanoprecipitation method, the PLGA nanoparticles prepared by the single emulsion method only have linear relationship ($D = 0.6244\ C + 9.4895$, $R^2 = 0.9676$) between the surface charge of nanoparticles and PLGA concentration. There is not obvious relationship between the particle size and PLGA concentration, similar to that reported in the literature. [35, 36] The discrepancy of the particle size could be explained by the high energy inhomogeneity provided by the sonic dismembrator. Accordingly, when the PLGA concentration changes, the organic phase (PLGA) will form nanoparticles with different and unpredictable sizes.

As described in Table 3-6, curcumin at a concentration of 10% of the PLGA concentration was added to these three formulations to further validate the size and surface charge of curcumin loaded PLGA nanoparticles are similar to those of blank PLGA nanoparticles. The curcumin loaded nanoparticles were 76.37 nm, 84.55 nm, and 86.05 nm in size, with -1.20 mV, -16.71 mV, and -43.04 mV surface charge, which reveals that no influence was exerted by curcumin on size and surface charge of PLGA nanoparticles. The loading and release behavior of curcumin loaded PLGA nanoparticle coated MEAs of these three formulations still requires further exploration and will be discussed in Chapter 5.

3.4 Conclusion

Using the nanoprecipitation method, the size and surface charge of PLGA nanoparticles can be precisely tailored by changing the surfactant and PLGA concentration within a specific PLGA concentration range. The relationships between PLGA concentration and the size and surface charge of PLGA nanoparticles can also provide guidance for the selection of an optimal curcumin loaded PLGA nanoparticle, because the addition of curcumin in the formulation has no effect on the particle size and surface charge. For the single emulsion method, increasing PLGA concentration will proportionally increase the net surface charge of PLGA nanoparticles. However, there is no obvious relationship or trend in the change of the PLGA nanoparticle size when the PLGA concentration is increased. The size of PLGA nanoparticles may depend more on the emulsification time and amplitude, which will be further explored in the next chapter.

CHAPTER 4: Bupivacaine hydrochloride loaded PLGA-PEG nanoparticles

4.1 Introduction

Pain management after surgery or injury requires the local anesthesia, and the local anesthetics need to possess some properties such as long drug duration and low toxicity. BUP stands out because of its nerve block and anti-inflammatory effects.[7-10, 37] However, free BUP has two potential shortcomings. One is that the analgesic effect of a single injection of BUP·HCl for nerve blockades or local infiltration typically lasts less than 24 hours, and the other is the requirement of catheter insertion, which is technically demanding and expensive, and usually accompanied with significant complications.[1, 38, 39] One solution is to load BUP·HCl onto the MEAs, because the MEAs can serve as a drug depot and has been proved to be an effective implantable device after SCI.[39-43] However, the coated MEA requires the loading agents to have specific physicochemical properties, lacks targeting and permeability to specific tissues and cells, and does not improve the cellular uptake and the extracellular matrix or intracellular diffusion of the drug.[44] Biodegradable polymeric nanoparticles are formulations with tailorable physicochemical properties. Thus, loading the therapeutic agent into the nanoparticle before coating on the MEA provides a method to overcome these shortcomings. In addition, biodegradable polymeric nanoparticles are also a good platform for sustained and controllable drug delivery, which may have promising future to further increase the drug loading and drug release duration of the nanoparticle-MEA combined drug delivery platform.

This chapter focuses on loading BUP·HCl into PLGA-PEG nanoparticles using emulsification solvent-evaporation method. The parameters such as emulsification time and amplitude will be explored to discover the effect on nanoparticle size. Also, after successfully loading BUP·HCl into PLGA-PEG nanoparticles, different BUP·HCl concentrations will be tested in order to confirm the optimal initial drug/polymer ratio for the highest drug loading.

4.2 Results

4.2.1 Effect of emulsification time and amplitude, and BUP·HCl concentration on the properties and drug loading of nanoparticles

Blank mPEG-PLGA (5k:45k, 50:50) nanoparticles were formulated using 20 mg mPEG-PLGA and 2% PVA, BUP·HCl loaded nanoparticles were prepared with 20 mg mPEG-PLGA, BUP·HCl at a concentration of 5% (w/w, 1 mg), 10% (w/w, 2 mg), 20% (w/w, 4 mg), or 40% (w/w, 8 mg) of the mPEG-PLGA concentration, and 2% PVA. All the nanoparticles were prepared by emulsification solvent-evaporation method, as described in Chapter 2.1. Specifically, four emulsification methods with different emulsification times and amplitudes, single emulsion under 10s emulsification time

and 20% amplitude, single emulsion under 30s emulsification time and 30% amplitude, double emulsion under 30s emulsification time and 20% amplitude in the first emulsification, and 30s emulsification time and 20% amplitude in the second emulsification, and double emulsion under 30s emulsification time and 30% amplitude in the first emulsification, and 30s emulsification time and 20% amplitude in the second emulsification, were tried. The particle size, PDI, zeta potential, drug loading, and drug encapsulation efficiency of the nanoparticles are listed in Table 4-1.

Table 4-1 BUP·HCl loaded mPEG-PLGA nanoparticles prepared with different emulsification parameters and BUP·HCl concentration

Emulsification method	Surfactant	BUP·HCl/ mPEG-PLGA ratio	Number Mean ± SEM (nm)	PDI ± SEM	Zeta Potential ± SEM (mV)
Single emulsion: 10s, 20% amplitude	2% PVA	Blank	105.31 ± 20.93	0.341 ± 0.030	-1.42 ± 0.08
		5%	114.41 ± 11.67	0.310 ± 0.032	-1.63 ± 0.15
		10%	172.43 ± 16.60	0.245±0.006	-1.57 ± 0.07
		20%	179.07 ± 4.53	0.223±0.002	-1.42 ± 0.17
		40%	149.66 ± 22.21	0.276 ± 0.032	-1.58 ± 0.30
Single emulsion: 30s,	2% PVA	Blank	136.73 ± 14.66	0.491 ± 0.050	-1.47 ± 0.13
		5%	119.04 ±14.67	0.351 ± 0.087	-1.64 ± 0.35

30% amplitude		10%	121.88 ± 4.72	0.345±0.047	-1.67 ± 0.10
		20%	113.65 ± 13.92	0.324±0.001	-1.88 ± 0.17
		40%	114.22 ± 13.88	0.348 ± 0.089	-1.81 ± 0.07
Double emulsion: 30s, 20% amplitude; 30s, 20% amplitude	2% PVA	Blank	93.03 ± 16.02	0.389±0.114	-2.82 ± 0.58
		5%	107.24 ± 5.26	0.395 ± 0.006	-1.84 ± 0.01
		10%	99.27 ± 12.33	0.204±0.003	-2.46 ± 0.05
		20%	105.31 ± 5.70	0.267±0.043	-2.88± 0.07
		40%	94.97 ± 17.44	0.281 ± 0.048	-2.67 ± 0.53
Double emulsion: 30s, 30% amplitude; 30s, 20% amplitude	2% PVA	Blank	91.44 ± 11.73	0.324±0.006	-1.54 ± 0.22
		5%	97.23 ± 21.55	0.248±0.001	-1.72 ± 0.01
		10%	114.14 ± 21.49	0.250±0.002	-1.92 ± 0.13

		20%	117.50 ± 9.18	0.246±0.019	-1.85 ± 0.23
		40%	112.68 ± 24.35	0.298 ± 0.006	-1.83 ± 0.12

Data are presented as average of N ≥ 3 batches. SEM: standard error of measurement

4.2.2 Relationship between BUP·HCl concentration and drug loading and drug encapsulation efficiency of nanoparticles

To visualize the relationship between BUP·HCl concentration and drug loading and drug encapsulation efficiency of nanoparticles, the relationship with constant emulsification parameters is presented in Figure 4-1.

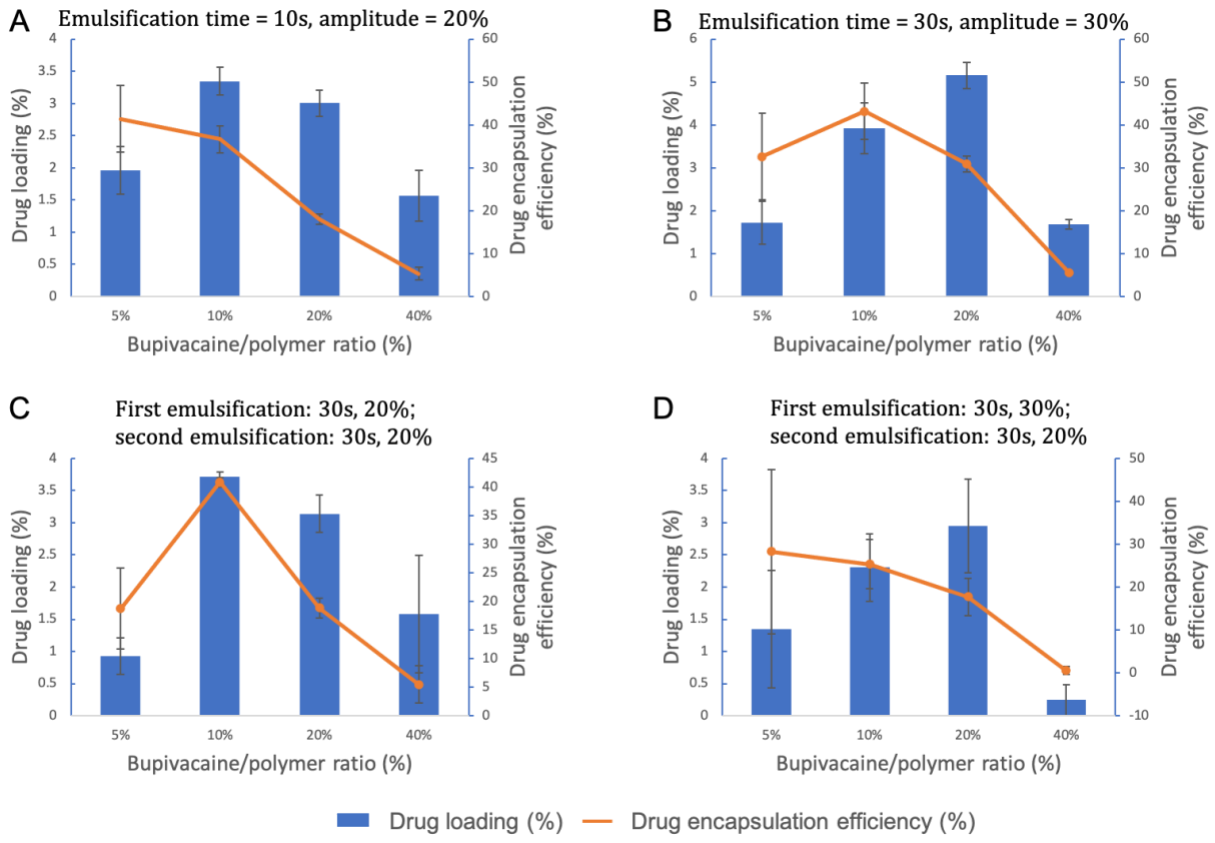

Figure 4-1 Relationship between BUP·HCl concentration and drug loading (blue bars) and drug encapsulation efficiency (orange line) of nanoparticles with different emulsification parameters: A) single emulsion: 10s emulsification time at 20% amplitude, B) single emulsion: 30s emulsification time at 30% amplitude, C) double emulsion: 30s emulsification time at 20% amplitude in the first emulsification, 30s emulsification time at 20% amplitude in the second emulsification, and D) double emulsion: 30s emulsification time at 30% amplitude in the first emulsification, 30s emulsification time at 20% amplitude in the second emulsification.

4.2.3 Relationship between emulsification method and drug loading and drug encapsulation efficiency of nanoparticles

To visualize the relationship between emulsification method and drug loading and drug encapsulation efficiency of nanoparticles, the relationship with constant BUP·HCl concentration is presented in Figure 4-2.

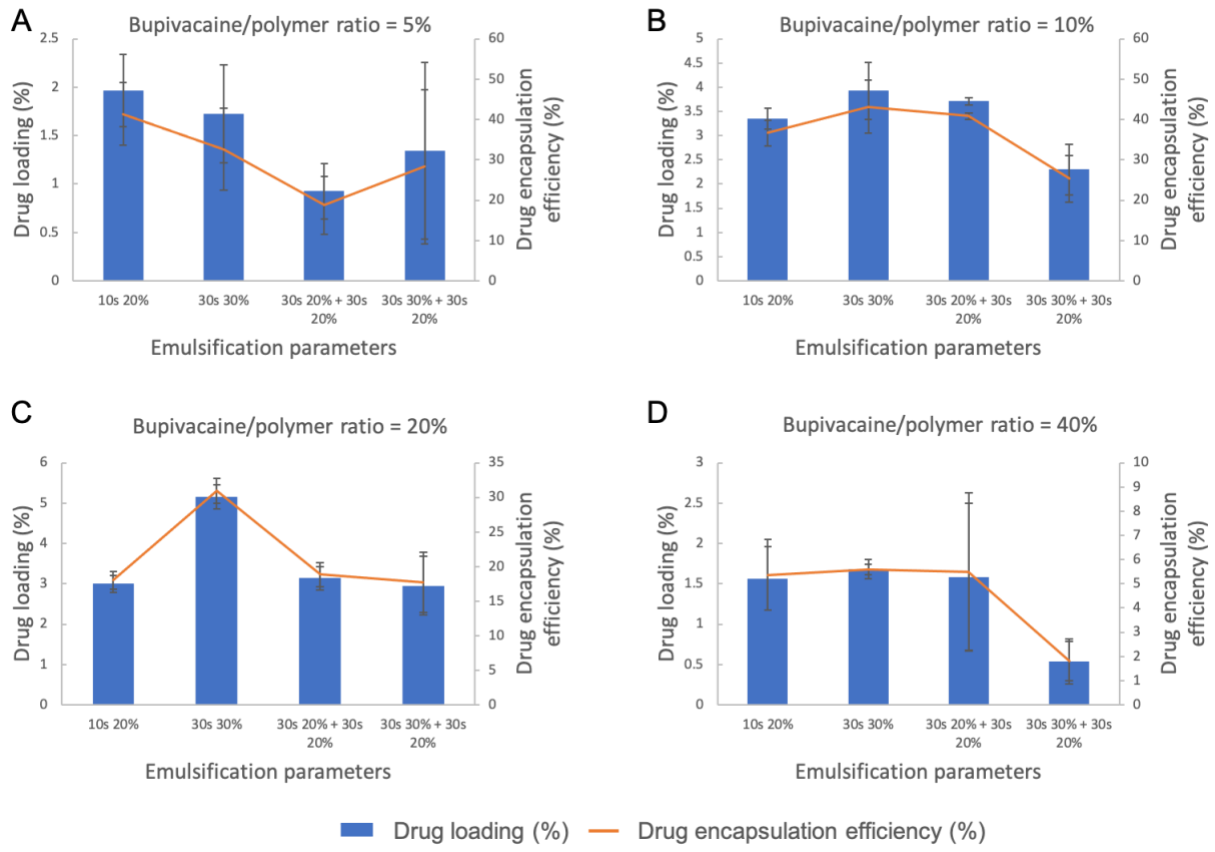

Figure 4-2 Relationship between emulsification parameters and drug loading (blue bars) and drug encapsulation efficiency (orange line) of nanoparticles with different BUP·HCl concentration: A) BUP·HCl/mPEG-PLGA = 5% (1 mg BUP·HCl), B) BUP·HCl/mPGE-PLGA = 10% (2 mg BUP·HCl), C) BUP·HCl/mPEG-PLGA = 20% (4 mg BUP·HCl), and D) BUP·HCl/mPEG-PLGA = 40% (8 mg BUP·HCl).

4.3 Discussion

In this chapter, the BUP·HCl loaded mPEG-PLGA nanoparticles with 2% PVA were formulated following the protocol (Chapter 2.2) adapted from the BUP·HCl loaded PLGA nanoparticle preparation protocols in the literature.[1, 23, 24, 45, 46] The effect of BUP·HCl concentration and emulsification parameters on size, surface charge, drug loading and drug encapsulation efficiency of nanoparticles were explored, while maintaining constant surfactant and mPEG-PLGA concentration.

Nanoparticles prepared by the single emulsion method under the conditions of 10s emulsification time and 20% amplitude are different in particle size from the nanoparticles prepared by the double emulsion method. In all other experiments, the particle size, PDI and surface charge of the remaining nanoparticles were not changed significantly, even if the BUP·HCl concentration and emulsification method were changed. Combined with the results in Chapter 3, one possible explanation is that the surfactant used in emulsification plays a more important role than the polymer concentration and emulsification time and amplitude. The difference between the size of the nanoparticles formulated with 3% CHA (Table S4-1) and the nanoparticles formulated with 2% PVA (Table 4-1) also provides support for this. Another potential explanation is that the emulsification conditions also have an effect on the particle size, herein, the difference is not significant because the emulsification conditions have not changed significantly - the size difference between the nanoparticles prepared under 30 s emulsification time and the nanoparticles prepared under 120 s emulsification time (Table S4-2) illustrates this point. However, the possibility that there is no trend between the emulsification conditions and the size of nanoparticles cannot be absolutely ruled out. Accordingly, more experiments with different emulsification times are required to draw a definitive conclusion. Additionally, there are still some variables that may affect the particle size in emulsification method, such as the concentration of the surfactant and the temperature of the sink condition, which require further exploration.[47, 48]

The BUP·HCl concentration in Figure 4-1 is in the range of 5% (1 mg BUP·HCl) to 40% (8 mg BUP·HCl). This data shows the drug encapsulation efficiency will decrease with the increase of BUP·HCl concentration, and the drug loading will first increase with the BUP·HCl concentration, then reach the critical point, after which the drug loading begins to decrease. These phenomena may be explained by the fact that some of the drug will be encapsulated inside the nanoparticle, and the rest of the drug may be absorbed onto the surface of the nanoparticle via physical absorption or remain in the sink. The amount of drug that can be encapsulated inside the nanoparticle is a constant when the size and shape of the nanoparticle and the solubility of the drug are constant. The amount of drug that can be physically absorbed on the surface of the nanoparticle is positively correlated with the concentration of the drug in a specific range of BUP·HCl concentration.[24]

According to Figure 4-2, the nanoparticles prepared by single emulsion method have a slightly higher drug loading and drug encapsulation efficiency, which may be attributed to the solubility of BUP·HCl. The volume of the aqueous solution to dissolve BUP·HCl in single emulsion method and double emulsion method is 4 mL and 0.2 mL, respectively, and it can be observed that there are BUP·HCl

chunks cannot be completely dissolved in the aqueous solution of double emulsion method. Therefore, the solubility of BUP·HCl can account for the slightly lower drug loading of nanoparticles prepared by double emulsion method. However, the p value ($p > 0.05$) indicates that there is no statistical relationship between drug loading and drug encapsulation efficiency and the emulsification conditions. In conclusion, the drug loading and drug encapsulation efficiency of BUP·HCl loaded mPEG-PLGA nanoparticles are not closely dependent on the emulsification conditions, but the effects of other formulation parameters such as surfactant need to be further explored. Furthermore, the formulation with about 20% BUP·HCl concentration will result in the highest drug loading amount, which can provide guidance for further research on formulation with other surfactants.

4.4 Conclusion

The size, PDI, surface charge, drug loading, and drug encapsulation efficiency of BUP·HCl loaded mPEG-PLGA nanoparticles are not closely related to the emulsification time and amplitude of emulsification solvent-evaporation method. The formulations using mPEG-PLGA (5k:45k) polymer will achieve the highest drug loading amount with a BUP·HCl concentration of approximately 20%. The formulation prepared by single emulsion method under the emulsification time of 30 s and the amplitude of 30% has a relatively high BUP·HCl loading. A BUP·HCl concentration of about 20% will result in a highest drug loading, and about 5% BUP·HCl can be loaded with this formulation protocol.

CHAPTER 5: Loading and release behavior of nanoparticles from the nanoparticle coated flexible microelectrode arrays

5.1 Introduction

The flexible MEA has been reported to be applied as a drug delivery device in some literature, and its capability to load polystyrene beads has been shown as well.[49-51] In order to achieve the nerve block effect, the flexible MEA is placed in the surgical drain after the spine surgery. However, if the therapeutic agent is directly loaded on the MEA, its permeability, diffusion and uptake rate will not be improved. Thus, negatively charged biodegradable nanoparticles are introduced. Additionally, the loading and release from the conductive polypyrrole films require physicochemical properties of the cargo that allow for drug loading and release upon electrical stimulation. Therefore, it is necessary to test the loading and release behavior of the nanoparticles, and find the optimal physicochemical properties of nanoparticles before finalizing the formulation protocol for BUP·HCl loaded nanoparticles.

In this chapter, fluorescence nanoparticles will be loaded and released from the MEAs in collaboration with Dr. Rajiv Saigal's group, who has developed the implantable flexible MEA technology. First, polystyrene beads are used as a control nanoparticle to test loading and release. Based on the polysystrene nanoparticle results and using findings from Chapter 3, CF555-labeled biodegradable nanoparticles with and without drug are formulated with different surface charges and are loaded into MEAs. Herein, curcumin is chosen as the model drug due to its high fluorescence intensity, which can be easily measured with a UV–Vis spectrometer. The relationship between the physicochemical properties of nanoparticles and the drug release behavior is measured and analyzed.

5.2 Results

5.2.1 Loading and release behavior of non-biodegradable nanoparticles

Fluorescence dye labeled 0.1 μm polystyrene beads (PS beads, ThermoFisher) were chosen as non-biodegradable nanoparticles based on polypyrrole-polystyrene coatings reported in literature.[50] The PS beads were diluted to 1% or 3%, loaded on the flexible MEA, and then released with or without application of direct current. Each MEA went through six washing cycles. The PS nanoparticle coated MEAs were imaged under the confocal microscope (Nikon Instruments) before the release process, and the released MEAs were imaged again. All the images were imaged under the same LUTs, and the fluorescence intensity was analyzed by Image J. The washing solution was collected and measured by SpectraMax M5 UV–Vis spectrometer at the range of 580 - 605 nm. The images of PS nanoparticle coated MEAs and analysis results are presented in Figure 5-1.

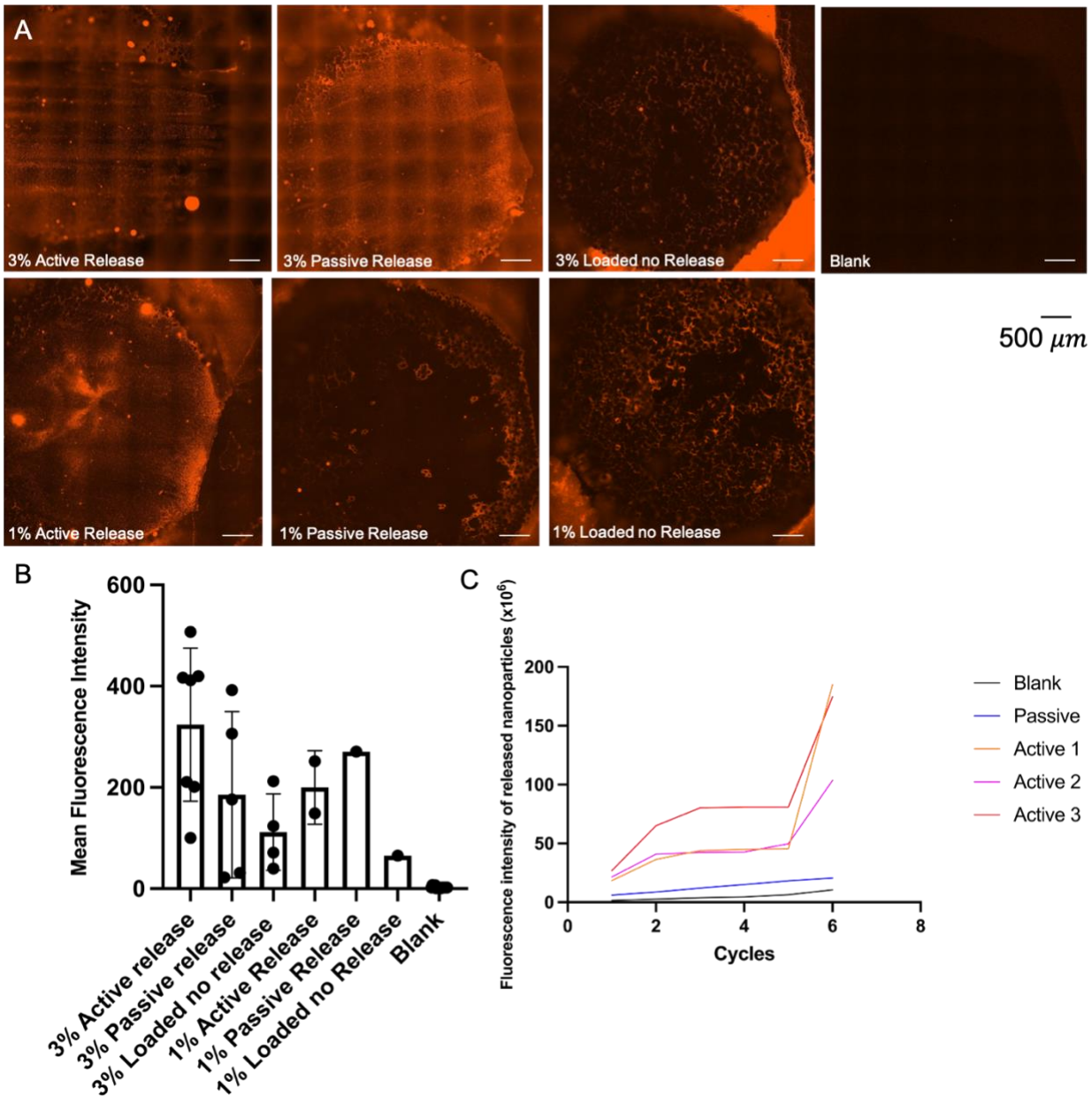

Figure 5-1 PS bead loaded and released electrodes. A) Confocal images of 3% and 1% PS beads coated MEAs undergone active release and passive release, PS beads coated MEA before undergoing release, and blank MEA, B) Mean fluorescence intensity of PS beads loaded/empty MEAs before/after release measured at the position 25 μm away from (z = 25 μm) the nanoparticle-MEA interface in z direction, C) PS beads have been released from the 3% PS bead loaded MEAs after each release-washing cycle.

5.2.2 Loading and release behavior of biodegradable nanoparticles

CF555 labeled PLGA and mPEG-PLGA polymers were used to prepare biodegradable nanoparticles, following the nanoprecipitation protocol described in Chapter 2.1. The biodegradable nanoparticles

were diluted to 10%, loaded on the flexible MEA, and then released with or without direct current. Each MEA went through three washing cycles. The biodegradable nanoparticle coated MEAs were imaged under the confocal microscope (Nikon Instruments) before the release process, and the released MEAs were imaged again. All the images were imaged under the same LUTs, and the fluorescence intensity were analyzed by Image J. The washing solution was collected and measured by SpectraMax M5 UV–Vis spectrometer. The images of PLGA nanoparticle coated MEAs and analysis results are presented in Figure 5-2.

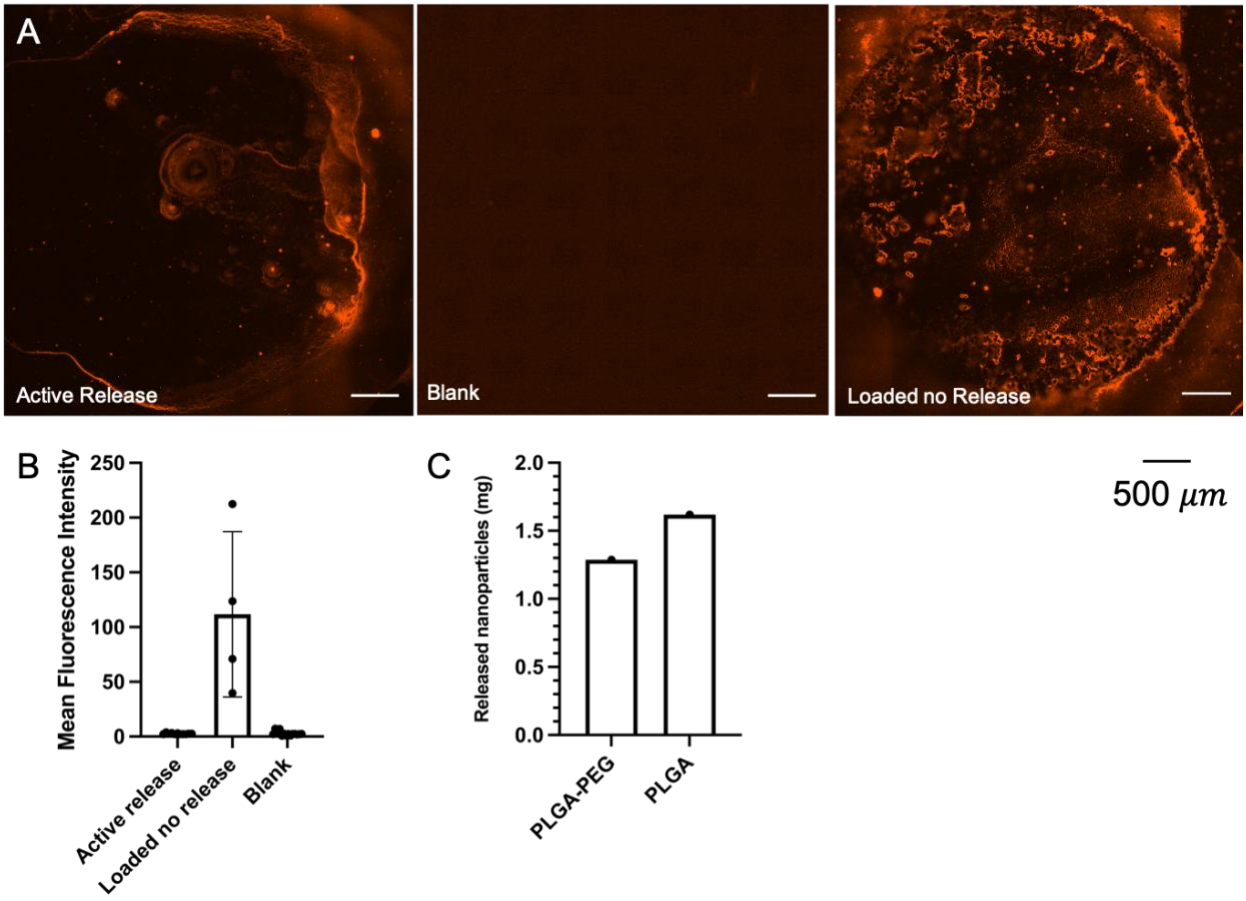

Figure 5-2 10% PLGA nanoparticle loaded and released electrodes. A) Confocal images of PLGA nanoparticles coated MEA undergone active release, Blank MEA, and PLGA nanoparticles coated MEA before undergoing release, B) Mean fluorescence intensity of PLGA nanoparticles loaded/empty MEAs before/after release measured at the position 25 μm away from (z = 25 μm) the nanoparticle-MEA interface in z direction, C) Biodegradable nanoparticles have been released via active release method after three release-washing cycles.

5.2.3 Release behavior of curcumin

Results above shown the biodegradable nanoparticles could be successfully loaded and released from the MEA, and nearly all the nanoparticles were released from the MEA after 3 washing cycles. Therefore, undiluted curcumin loaded PLGA nanoparticles with different surface charge (Chapter 3.2.2.5) were loaded to study the drug release behavior. The released curcumin in the washing solution was quantified after each washing cycle using SpectraMax M5 UV–Vis spectrometer. The release profile of curcumin is presented in Figure 5-3.

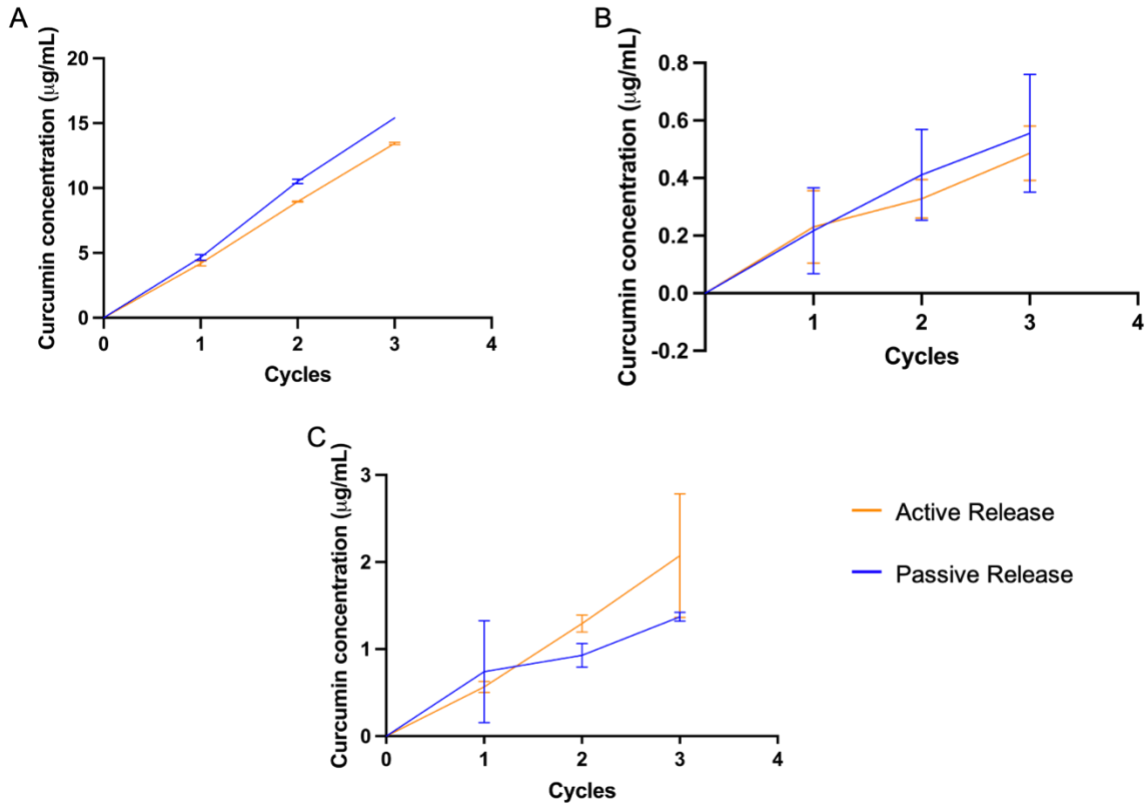

Figure 5-3 Curcumin and curcumin loaded PLGA nanoparticle release from the curcumin loaded PLGA nanoparticle-polypyrrole coated MEA. A) Curcumin loaded PLGA nanoparticles with near neutral surface charge (prepared with 2% PVA), B) Curcumin loaded PLGA nanoparticles with negative surface charge (prepared with 5% F68), and C) Curcumin loaded PLGA nanoparticles with high negative surface charge (prepared with 3% CHA)

5.3 Discussion

The confocal images of PS bead loaded MEAs show that 0.1 μm PS beads can be successfully loaded and released from the PS bead-polypyrrole coating on the MEA, and the PS beads would not aggregate on the polypyrrole coating when the current was applied. In addition, the fluorescence intensity

quantification study of the washing solution shows that the release of PS beads is controllable by applying the direct current. These results provide foundation for loading and release of biodegradable nanoparticles.

The biodegradable nanoparticles can also be successfully loaded and released from the biodegradable nanoparticle-polypyrrole coating on the MEA, and no obvious aggregations were observed as well. However, the confocal images of the MEAs after 3 active release cycles indicate that almost all the biodegradable nanoparticles were released within 3 release-washing cycles. One potential explanation is that the release behavior of nanoparticles depends on the surface charge. To validate this hypothesis, curcumin loaded PLGA nanoparticles with different surface charge were loaded and released from the MEA.

Among the three formulations, PLGA nanoparticles with a surface charge close to neutral have the fastest release speed, and negatively charged PLGA nanoparticles have the slowest release speed. The release speed of highly negatively charged PLGA nanoparticles is somewhere in between. This may be attributed to the electrical properties of polypyrrole. However, there is no obvious difference in the release profiles was observed between the active release method and passive release method. Also, despite the high concentration of nanoparticles, only very low fluorescence intensity was detected in all washing solutions. This is probably caused by the aggregation of curcumin loaded nanoparticles. Curcumin may interact with pyrrole during the loading process and then induce the aggregation of nanoparticles, because there are aggregates can be observed on the top of the MEA (Figure S5-1) and the released curcumin loaded PLGA nanoparticle increased when the coating did not contain pyrrole (Figure S5-2). To further figure out whether curcumin is the cause of aggregation, and to explore the relationship between the release behavior of nanoparticles and the surface charge of nanoparticles, another fluorescence dye, Rhodamine B instead of curcumin will be encapsulated in biodegradable nanoparticles with different surface charge to continue the release study.

5.4 Conclusion

Loading and releasing nanoparticles from the MEA is feasible, but the relationship between the surface charge of nanoparticles and nanoparticle release behavior needs further exploration. Additionally, the interaction between the drug in the nanoparticles and the pyrrole used for MEA coating is still unclear. In further study, the interaction between curcumin and the polypyrrole coating will be determined first. Then the relationship between the surface charge of PLGA nanoparticles and release behavior of PLGA nanoparticles will be explored. Once the optimal physicochemical properties of nanoparticles are finalized, based on the studies of relationship

between the formulation parameters and the physicochemical properties of nanoparticles (Chapter 3, Chapter 4), the BUP·HCl loaded nanoparticles will be formulated in a short period of time. Thereafter, the efficacy study of the BUP·HCl loaded nanoparticle-polypyrrole coated MEA will be conducted.

BIBLIOGRAPHY

1. Zhang, W.J., et al., *Precision-guided long-acting analgesia by Gel-immobilized bupivacaine-loaded microsphere.* Theranostics, 2018. **8**(12): p. 3331-3347.
2. Santamaria, C.M., et al., *Drug delivery systems for prolonged duration local anesthesia.* Materials Today, 2017. **20**(1): p. 22-31.
3. Ingadottir, B., et al., *Development, Usability, and Efficacy of a Serious Game to Help Patients Learn About Pain Management After Surgery: An Evaluation Study.* JMIR Serious Games, 2017. **5**(2): p. e10.
4. Hah, J.M., et al., *Chronic Opioid Use After Surgery: Implications for Perioperative Management in the Face of the Opioid Epidemic.* Anesth Analg, 2017. **125**(5): p. 1733-1740.
5. Balocco, A.L., et al., *Extended release bupivacaine formulations for postoperative analgesia: an update.* Curr Opin Anaesthesiol, 2018. **31**(5): p. 636-642.
6. Chahar, P. and K.C. Cummings, 3rd, *Liposomal bupivacaine: a review of a new bupivacaine formulation.* J Pain Res, 2012. **5**: p. 257-64.
7. Wang, J., N. Wang, and F.H. Gong, *Efficacy of bupivacaine infiltration for controlling post-tonsillectomy pain, duration of surgery and post-operative morbidities: A systematic review and meta-analysis.* Experimental and Therapeutic Medicine, 2021. **21**(3).
8. Block, L., et al., *Ultralow concentrations of bupivacaine exert anti-inflammatory effects on inflammation-reactive astrocytes.* Eur J Neurosci, 2013. **38**(11): p. 3669-78.
9. Hansson, E. and E. Skioldebrand, *Anti-inflammatory effects induced by ultralow concentrations of bupivacaine in combination with ultralow concentrations of sildenafil (Viagra) and vitamin D3 on inflammatory reactive brain astrocytes.* PLoS One, 2019. **14**(10): p. e0223648.
10. Behnaz, F., et al., *Sympatholytic and Anti-Inflammatory Effects of Ropivacaine and Bupivacaine After Infraclavicular Block in Arterio Venous Fistula Surgery.* Anesth Pain Med, 2019. **9**(1): p. e85704.
11. Kumari, A., S.K. Yadav, and S.C. Yadav, *Biodegradable polymeric nanoparticles based drug delivery systems.* Colloids Surf B Biointerfaces, 2010. **75**(1): p. 1-18.
12. Chan, J.M., et al., *Polymeric nanoparticles for drug delivery.* Methods Mol Biol, 2010. **624**: p. 163-75.
13. Kim, Y.H., et al., *Robust and real-time monitoring of nerve regeneration using implantable flexible microelectrode array.* Biosensors & Bioelectronics, 2009. **24**(7): p. 1883-1887.
14. McAvoy, M.B., B.D. Choi, and P.S. Jones, *Immune Therapy for Central Nervous System Metastasis.* Neurosurg Clin N Am, 2020. **31**(4): p. 627-639.
15. Meng, F.S., et al., *Polymeric-based microneedle arrays as potential platforms in the development of drugs delivery systems.* Journal of Advanced Research, 2020. **26**: p. 137-147.
16. Rui, Y.F., et al., *Parylene-based implantable Pt-black coated flexible 3-D hemispherical microelectrode arrays for improved neural interfaces.* Microsystem Technologies-Micro-and Nanosystems-Information Storage and Processing Systems, 2011. **17**(3): p. 437-442.
17. Yi, W.W., et al., *A flexible and implantable microelectrode arrays using high-temperature grown vertical carbon nanotubes and a biocompatible polymer substrate.* Nanotechnology, 2015. **26**(12).
18. Guo, R. and J. Liu, *Implantable liquid metal-based flexible neural microelectrode array and its application in recovering animal locomotion functions.* Journal of Micromechanics and Microengineering, 2017. **27**(10).
19. Valdes-Ramirez, G., et al., *Multiplexed and switchable release of distinct fluids from microneedle platforms via conducting polymer nanoactuators for potential drug delivery.* Sensors and Actuators B-Chemical, 2012. **161**(1): p. 1018-1024.

20. Huang, Y., et al., *Nanostructured Polypyrrole as a flexible electrode material of supercapacitor.* Nano Energy, 2016. **22**: p. 422-438.
21. Spearman, B.S., et al., *Conductive interpenetrating networks of polypyrrole and polycaprolactone encourage electrophysiological development of cardiac cells.* Acta Biomater, 2015. **28**: p. 109-120.
22. Xu, Q., et al., *Scalable method to produce biodegradable nanoparticles that rapidly penetrate human mucus.* J Control Release, 2013. **170**(2): p. 279-86.
23. Alejo, T., et al., *Controlled release of bupivacaine using hybrid thermoresponsive nanoparticles activated via photothermal heating.* Journal of Colloid and Interface Science, 2018. **523**: p. 234-244.
24. Park, S.Y., et al., *Synthesis and Characterization of Polyfumarateurethane Nanoparticles for Sustained Release of Bupivacaine.* Pharmaceutics, 2020. **12**(3).
25. Foged, C., et al., *Particle size and surface charge affect particle uptake by human dendritic cells in an in vitro model.* Int J Pharm, 2005. **298**(2): p. 315-22.
26. He, C., et al., *Effects of particle size and surface charge on cellular uptake and biodistribution of polymeric nanoparticles.* Biomaterials, 2010. **31**(13): p. 3657-66.
27. Park, Y.H., et al., *Effect of the size and surface charge of silica nanoparticles on cutaneous toxicity.* Molecular & Cellular Toxicology, 2013. **9**(1): p. 67-74.
28. Jun, S.H., et al., *Synthesis of Retinol-Loaded Lipid Nanocarrier via Vacuum Emulsification to Improve Topical Skin Delivery.* Polymers (Basel), 2021. **13**(5).
29. Guillot, A.J., et al., *Cyanocobalamin Ultraflexible Lipid Vesicles: Characterization and In Vitro Evaluation of Drug-Skin Depth Profiles.* Pharmaceutics, 2021. **13**(3).
30. Ilic, K., et al., *Interaction of Differently Coated Silver Nanoparticles With Skin and Oral Mucosal Cells.* J Pharm Sci, 2021.
31. Yamada, Y., G. Fichman, and J.P. Schneider, *Serum Protein Adsorption Modulates the Toxicity of Highly Positively Charged Hydrogel Surfaces.* ACS Appl Mater Interfaces, 2021. **13**(7): p. 8006-8014.
32. Yadav, S.P.S., et al., *Mechanism of how carbamylation reduces albumin binding to FcRn contributing to increased vascular clearance.* Am J Physiol Renal Physiol, 2021. **320**(1): p. F114-F129.
33. Alnasser, Y., et al., *Preferential and Increased Uptake of Hydroxyl-Terminated PAMAM Dendrimers by Activated Microglia in Rabbit Brain Mixed Glial Culture.* Molecules, 2018. **23**(5).
34. Joseph, A., et al., *Curcumin-loaded polymeric nanoparticles for neuro-protection in neonatal rats with hypoxic-ischemic encephalopathy.* Nano Research, 2018. **11**(10): p. 5670-5688.
35. Xie, S., et al., *Effect of PLGA as a polymeric emulsifier on preparation of hydrophilic protein-loaded solid lipid nanoparticles.* Colloids Surf B Biointerfaces, 2008. **67**(2): p. 199-204.
36. Hernandez-Giottonini, K.Y., et al., *PLGA nanoparticle preparations by emulsification and nanoprecipitation techniques: effects of formulation parameters.* Rsc Advances, 2020. **10**(8): p. 4218-4231.
37. Gercek, A., et al., *The analgesic and anti-inflammatory effects of subcutaneous bupivacaine, morphine and tramadol in rats.* Agri, 2004. **16**(3): p. 53-8.
38. Dinges, H.C., et al., *The analgesic efficacy of liposomal bupivacaine compared with bupivacaine hydrochloride for the prevention of postoperative pain: a systematic review and meta-analysis with trial sequential analysis.* Reg Anesth Pain Med, 2021.
39. Xie, X., et al., *Analgesic Microneedle Patch for Neuropathic Pain Therapy.* ACS Nano, 2017. **11**(1): p. 395-406.
40. Gutierrez-Martinez, J., et al., *Neuroprosthesis Devices Based on Micro- and Nanosensors: A Systematic Review.* Journal of Sensors, 2020. **2020**.
41. Kilgore, K.L., et al., *Powering strategies for implanted multi-function neuroprostheses for spinal cord injury.* Healthcare Technology Letters, 2020. **7**(3): p. 81-86.

42. Cai, H.T., et al., *Low pressure voiding induced by a novel implantable pudendal nerve stimulator.* Neurourology and Urodynamics, 2019. **38**(5): p. 1241-1249.
43. Shepherd, R.K., et al., *The development of neural stimulators: a review of preclinical safety and efficacy studies.* Journal of Neural Engineering, 2018. **15**(4).
44. Gill, H.S. and M.R. Prausnitz, *Coating formulations for microneedles.* Pharmaceutical Research, 2007. **24**(7): p. 1369-1380.
45. Ning, C., et al., *On-Demand Prolongation of Peripheral Nerve Blockade through Bupivacaine-Loaded Hydrogels with Suitable Residence Periods.* Acs Biomaterials Science & Engineering, 2019. **5**(2): p. 696-709.
46. Ma, P.J., et al., *Local anesthetic effects of bupivacaine loaded lipid-polymer hybrid nanoparticles: In vitro and in vivo evaluation.* Biomedicine & Pharmacotherapy, 2017. **89**: p. 689-695.
47. Kwon, H.Y., et al., *Preparation of PLGA nanoparticles containing estrogen by emulsification-diffusion method.* Colloids and Surfaces a-Physicochemical and Engineering Aspects, 2001. **182**(1-3): p. 123-130.
48. Kim, J.H., et al., *Preparation of PLGA nanoparticles containing estrogen by modified emulsification-diffusion method.* Abstracts of Papers of the American Chemical Society, 2001. **221**: p. U440-U440.
49. Kojabad, Z.D. and S.A. Shojaosadati, *Chemical synthesis of polypyrrole nanostructures: Optimization and applications for neural microelectrodes.* Materials & Design, 2016. **96**: p. 378-384.
50. Castagnola, E., et al., *Multilayer poly(3,4-ethylenedioxythiophene)-dexamethasone and poly(3,4-ethylenedioxythiophene)-polystyrene sulfonate-carbon nanotubes coatings on glassy carbon microelectrode arrays for controlled drug release.* Biointerphases, 2017. **12**(3).
51. Zhou, T., et al., *Guided Electrokinetic Assembly of Polystyrene Microbeads onto Photopatterned Carbon Electrode Arrays.* Acs Applied Materials & Interfaces, 2020. **12**(31): p. 35647-35656.

APPENDIX A: Supplementary Tables to Chapter 4

Table S4-1 mPEG-PLGA nanoparticles prepared with 3% CHA by single emulsion method

Polymer concentration (mg/mL)	BUP·HCl concentration (mg/mL)	Number Mean ± SEM (nm)	PDI ± SEM	Zeta Potential ± SEM (mV)
20	0	62.17 ± 0.36	0.216 ± 0.017	-3.58 ± 0.94
20	4	65.80 ± 1.59	0.277 ± 0.007	-3.66 ± 0.27

Data are presented as average of N = 3 batches. SEM: standard error of measurement

Table S4-2 PLGA nanoparticles prepared with 2% PVA by single emulsion method under 30% amplitude

Polymer concentration (mg/mL)	Emulsification time (s)	Number Mean ± SEM (nm)	PDI ± SEM	Zeta Potential ± SEM (mV)
20	30	80.84 ± 16.43	0.340 ± 0.032	-0.53 ± 0.057
20	120	56.19 ± 12.80	0.291 ± 0.035	-8.05 ± 0.54

Data are presented as average of N = 3 batches. SEM: standard error of measurement

APPENDIX B: Supplementary Tables to Chapter 5

Table S5-1 CF555 labeled biodegradable nanoparticles

Polymer	Surfactant	Number Mean ± SEM (nm)	PDI ± SEM	Zeta Potential ± SEM (mV)
PLGA (45k)	1% P80	91.89 ± 9.49	0.160 ± 0.034	-16.63 ± 8.04
mPEG-PLAG (5k:45k)	N/A	64.45 ± 1.60	0.191 ± 0.015	-5.28 ± 1.14

Data are presented as average of N = 3 batches. SEM: standard error of measurement

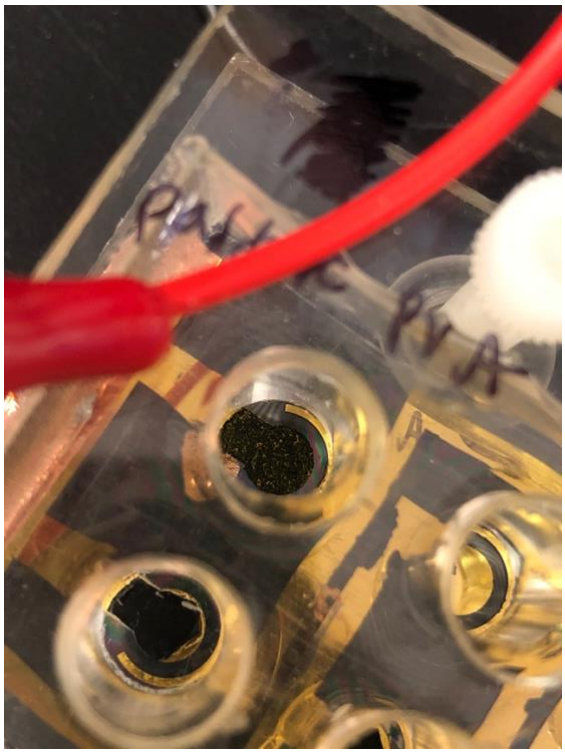

Figure S5-1 Curcumin loaded PLGA nanoparticle-polypyrrole coated MEA

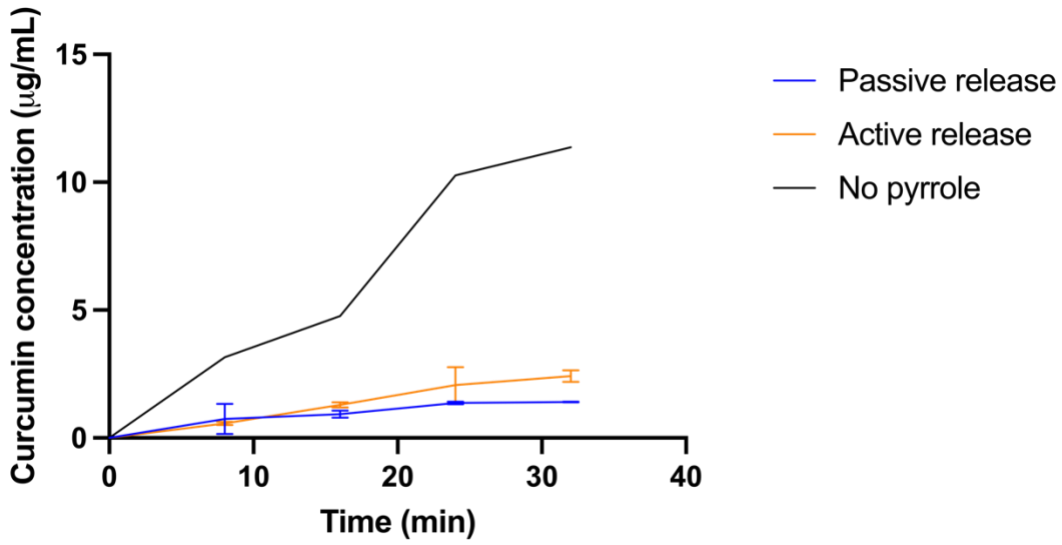

Figure S5-2 Curcumin loaded nanoparticles released from the curcumin loaded PLGA nanoparticle-polypyrrole coated MEA. Curcumin loaded PLGA nanoparticles were prepared with 3% CHA.